NUMERICAL STUDY OF BLOCK TEARING FAILURE IN STEEL ANGLES CONNECTED BY ONE LEG

E. BERNATOWSKA[1], L. ŚLĘCZKA[2]

Block tearing is a failure mode of steel connections based on rupture of material. In this paper, a numerical model is developed to capture fracture initiation and progression until failure in steel angles connected by one leg using single row of bolts. It was realized using Gurson-Tvergaard-Needleman porous material model, which can accurately trace the behaviour of steel at plastic and ultimate range. Obtained results are validated on laboratory test results in global and local terms. Stress distribution along the failure paths in the gross and net area subjected to shear and tension was investigated for different geometrical arrangements of connections. Observation of rupture mechanisms allowed to compare the design procedures given in Eurocode 3 with connections behaviour. Results of analysis indicate that both plastic stress distribution in gross shear area and ultimate stress distribution in net shear area can limit block tearing resistance, which is consistent with the newest code provisions.

Keywords: *bolted connections, block shear, numerical analysis, Gurson-Tvergaard-Needleman material model, steel angles*

---

[1] DSc., Eng., Rzeszow University of Technology, Faculty of Civil and Environmental Engineering and Architecture, Poznanska 2 Street, 35-084 Rzeszow, Poland, e-mail: e_bernat@prz.edu.pl

[2] DSc., PhD., Eng., Rzeszow University of Technology, Faculty of Civil and Environmental Engineering and Architecture, Poznanska 2 Street, 35-084 Rzeszow, Poland, e-mail: sleczka@prz.edu.pl

1. INTRODUCTION

Block tearing (or block shear) in steel bolted connections is a limit state based on simultaneous tension rupture along one path and shear yielding, or shear rupture, along another path [3]. Longitudinal shear and perpendicular tension failure paths occur in bolt lines, where bolt holes weaken the gross section of connected member, (Fig. 1). The influence of block tearing on connection resistance is compounded by the close spacing of bolts. It minimizes the length of the connection, but also decreases the net area subjected to shear $A_{nv.}$

Although block shear tearing was first identified relatively recently by Birkemoe and Gilmor [2] in coped beams, there have been many laboratory tests to experimentally predict such behaviour of steel angles connected by one leg, e.g. [10-12, 14, 15], and to formulate adequate strength functions, but finite element analyses of block shear failure phenomena in such joints are not numerous. This is due to the difficulties in destruction processes modelling, which require an appropriate material model capturing the plastic fracture process. Previously conducted analyses on angles connected by one leg [10, 13, 16] were to some extent simplified. In most of them linear elastic – non-linear hardening material models were used and fracture determination was usually based on reaching the specified value of plastic strain at reference point, which does not allow sufficient redistribution of stresses to appear prior to failure. Some of the numerical simulations took into account the way of load transfer by bolts in bearing in a simplified manner (by coupling one-half of the circumference of each bolt hole on steel member with the opposite face of gusset plate). In some cases shell elements were used. Such limitations in modelling capabilities were employed to reduce required computational time.

Recently, very sophisticated numerical studies of block shear have been carried out, but they are limited to rectangular gusset plate connections or coped beam connections [5, 17].

This paper focuses on numerical analysis of steel angles connected by one leg using single row of bolts. Numerical model is developed to capture the rupture initiation and progression until failure and to consider contact conditions between all components (angle, bolts and gusset plate). Such approach allows of load transfer by direct bearing of bolts. Extensive parametric analyses were conducted using porous material (Gurson-Tvergaard-Needleman) model. It takes into account the influence of microstructural damage on the material strength and the load capacity. Obtained results allow to compare the design procedures given in EN 1993-1-8 [3] and in its new version prEN 1993-1-8:2019 [4] with observed behaviour of connections.
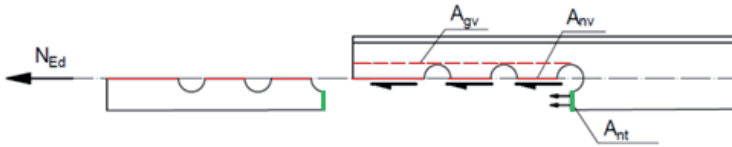
Fig. 1. Schema of block tearing in steel angle member connected by one leg

2. BLOCK TEARING RESISTANCE ACCORDING TO EUROCODE 3

When calculating tensile resistance of angle members connected by one leg, code regulations require checking ultimate resistance of net cross section as well as block tearing resistance. Current version of EN 1993-1-8 [3] gives two formulas to calculate the second one: for a symmetric bolt group subjected to concentric loading - Eq. (2.1) and for a bolt group subjected to eccentric loading - Eq. (2.2).

(2.1)
$$V_{eff,1,Rd} = f_u A_{nt} / \gamma_{M2} + \left(1/\sqrt{3}\right) f_y A_{nv} / \gamma_{M0}$$

(2.2)
$$V_{eff,2,Rd} = 0.5 f_u A_{nt} / \gamma_{M2} + \left(1/\sqrt{3}\right) f_y A_{nv} / \gamma_{M0}$$

where: A_{nt} – net area subjected to tension, A_{nv} – net area subjected to shear (Fig. 1), f_y – yield stress, f_u – tensile strength of steel, γ_{M0} and γ_{M2} – partial factors equal to 1.0 and 1.25 respectively.

However, new version of Eurocode is being prepared [4]. It also proposes two different formulas for block tearing resistance with some changes: for a bolt group where the tension stress on the tension area is uniform - Eq. (2.3) and for a bolt group where the tension stress on the tension area is non-uniform – Eq. (2.4).

(2.3)
$$V_{eff,1,Rd} = \left[A_{nt} f_u + \min\left(\frac{A_{gv} f_y}{\sqrt{3}}; \frac{A_{nv} f_u}{\sqrt{3}} \right) \right] / \gamma_{M2}$$

(2.4)
$$V_{eff,2,Rd} = \left[0.5 A_{nt} f_u + \min\left(\frac{A_{gv} f_y}{\sqrt{3}}; \frac{A_{nv} f_u}{\sqrt{3}} \right) \right] / \gamma_{M2}$$

where: A_{gv} – gross area subjected to shear (Fig. 1).

Tension angle members connected by one leg are included in the first group according to [4], while current version of EN 1993-1-8 [3] does not say precisely which equation should be used for such case.

3. FINITE ELEMENT MODELLING

3.1. MATERIAL MODEL DESCRIPTION

The porous metal plasticity was implemented using Gurson-Tvergaard-Needelman (GTN) material model. Due to such approach, damage of the material microstructure was taken into account. The process of material destruction depends not only on effective stress measure (according to Huber-Mises-Hencky hypothesis), but also on the hydrostatic part of the stress components, yield stress of material and on modified void volume fraction. When the material is not subjected to the loading, modified void volume fraction is equal to the initial value f_0, which is a basic GTN material parameter. During increase of loading, modified void volume fraction is approaching to the level when voids coalescence starts (f_c) until it reaches value corresponding to the complete loss of the material strength, at final separation of the material (f_F). The damage evolution is described by f_N, ε_N and s_N parameters. The presence of the voids in material and other parameters are constant values and depend only on the structure of the material. They should be identified for considered material.

Such process and GTN material capabilities are described extensively in [1, 7-9]. Used mechanical properties of steel were obtained from tensile tests of standard coupons cut from angle legs made of steel with nominal grade S275 and were equal to $f_y = 288$ MPa, $f_u = 425$ MPa. Other parameters which determine the process of material failure in the GTN material model were obtained from available literature [7-9] and from calibration process based on own experimental research [1]. The microstructural parameters of the GTN material model employed in simulations are presented in Table 1.

Table 1. The microstructural parameters of the GTN material model

Steel grade	f_0	q_i	f_c	f_F	f_N	ε_N	s_N
S275	0.001	q_1=1.5 q_2=1.0 q_3=2.25	0.06	0.2	0.02	0.3	0.1

3.2. BUILDING OF BOLTED JOINT FE MODEL

Employed FE models were developed using the ABAQUS software. They included four components: angle, gusset plate, bolts with nuts and washers. Due to the symmetry and to save calculation time, only half of each specimen was modelled. The load in z-direction was applied to the gusset plate in the form of prescribed displacement. The end of angle (plane of symmetry) could not move in z-direction. Initially both washers and bolts were located concentrically with holes' axes in angle and gusset plate. The picture below (Fig. 2) presents the view on complete model with the finite elements mesh and applied boundary condition.
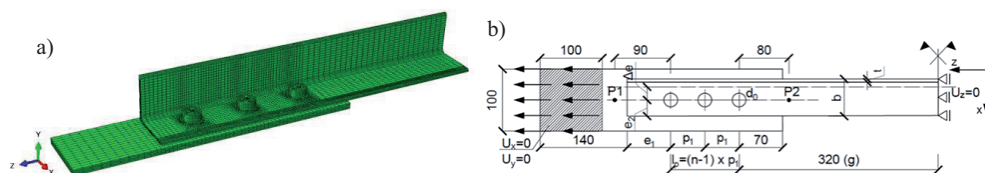

Fig. 2. Angle member connected by one leg: a) FE model, b) geometry and boundary conditions

Linear elastic – non-linear hardening material models based on coupon-test results were implemented for gusset plate and bolts (class 10.9). For the whole angle member, where fracture was expected, GTN material model was applied. Implementation of porous material model required carrying Dynamic Explicit analysis. For angles, gusset plates and washers, C3D8R type of element was employed. It is defined as a three-dimensional, hexahedral 8-node linear brick with reduced integration. This type of element has proved to be suitable when simulating lap bolted connections [13]. Bolt's shanks were modelled without the thread, as smooth cylinders with diameter equal to the nominal diameter of the bolt. They were built by using C3D8T and C3D6T elements, which are respectively 8-node thermally, coupled bricks with trilinear displacement and temperature and 6-node thermally coupled triangular prism used to complete the mesh. To apply a small clamping force starting from snug-tightened bolts, the vertical thermal deformation method was utilised [6]. Contact between surfaces was defined using general contact option. Frictional effects between the surfaces were also included by incorporating the classical isotropic Coulomb friction model in the contact definition, with a friction coefficient μ equal to 0.1.

3.3. VALIDATION OF NUMERICAL MODELS WITH 2, 3 OR 4 BOLTS

The first stage of computational model hierarchical validation was described in [1]. It included tests on single plates with drilled holes and tests on angles connected by one bolt to the gusset plates. The final stage of validation included connections with 2, 3 or 4 bolts. Its range is presented in Table 2.

Table 2. The range of experimental tests compared with FE modelling

Specimen designation	Profile	Bolts	e_1 [mm]	p_1 [mm]	e_2 [mm]	$N_{ult,Exp}$ [kN] (1)	$N_{ult,FEA}$ [kN] (2)	(2)/(1)
J8/3/55/40	L80x6	3×M20	70	55	40	242.1	248.1	1.02
J8/4/55/40	L80x6	4×M20	70	55	40	268.6	283.8	1.06
J6/2/90/34	L60x6	2×M16	55	90	34	218.2	214.3	0.98
J6/2/45/25	L60x6	2×M16	55	45	25	138.6	140.8	1.02
J6/3/45/25	L60x6	3×M16	55	45	25	180.7	184.4	1.02

Comparisons between tests and numerical analysis included load versus displacement curves F-Δ, out-of-plane deflections of angles, distribution and progress of strains during loading in chosen cross sections, fracture sequence and final fracture profiles. Both ultimate resistance obtained from tests $N_{ult,Exp}$ and from FE analysis $N_{ult,FEA}$ were considered as the maximum load level of the load-displacement path. Comparison of the computed F-Δ curve with these from experiment is depicted in Fig. 3 for one of the specimens. Quite good accuracy has been observed in terms of resistance for all validated specimens – mean value of $N_{ult,FEA}$ / $N_{ult,Exp}$ ratio is equal to 1.02 (see Table 2). Comparisons between the numerical and experimental shape of fracture correlated well. The model was not weakened in any way in this region to enable the development of failure mode. In all specimens fracture occurred in net area subjected to tension, which was followed by drop in F-Δ path, (Fig. 3). Fracture in shear area was not observed – it can be explained by domination of bending behaviour after rupture of tension net area.
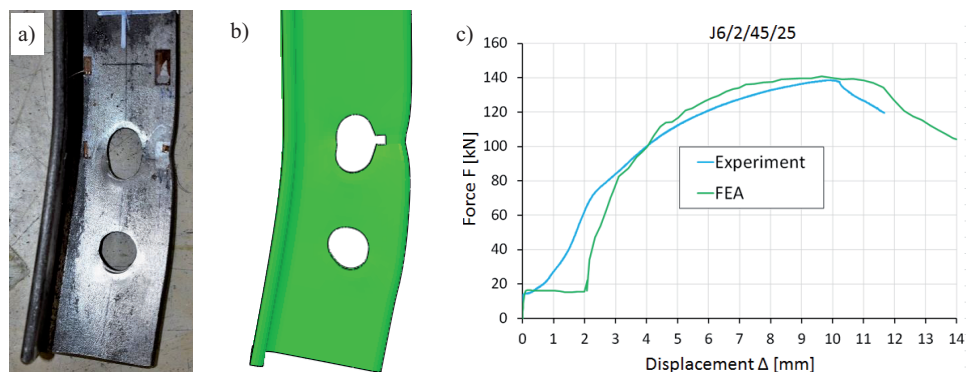
Fig. 3. Specimen J6/2/45/25: a) failure initiation obtained in the experimental test, b) visible symptom of fracture initiation in FE model, c) comparison of obtained force-displacement curves.

3.4. SCOPE OF THE FE ANALYSIS

To determine the impact of individual geometrical parameters on the global behaviour of the steel angle joints and their resistance, parametric analysis was carried out. Fifty-eight numerical models were built, divided into 5 groups (A1 ÷ A5), where following parameters were investigated:

- the ratio of the width of the leg to its thickness b/t (slenderness of the angle walls), in equal leg angles (A1),
- the spacing between centres of bolt holes in a line of load transfer p_1 and the total length of the connection l_p (A2),
- the edge distance from the centre of a fastener hole to the adjacent edge of angle, measured at right angles to the direction of load transfer e_2 (A3),
- the end distance from the centre of a fastener hole to the adjacent end of angle, measured in the direction of load transfer e_1 (A4),
- profile arrangement for unequal-leg angles (connections made by its wider or smaller leg (A5)).

Mentioned parameters are illustrated in Fig. 2b. The gusset plate thickness was equal to 10 mm. Reference points P1 and P2 were used to determine longitudinal displacement. Number of bolts varied in the range n = 1 ÷ 5. Nominal diameter of used bolts was M20. Models of connection were created in a such way, to cause only angle member failure. The resistances of bolts and gusset plate were greater than expected tensile resistance of the angle member (bolts class 10.9 were used). The analysis took into account the sizes of angles produced in the steel mills. Also several cross-sections were created only for the purpose of analysis, to obtain extreme geometrical proportions of both the angles

cross-section and the connection. Thanks to this, "model similarity" was achieved to the entire population of angle profiles of various sizes, connected with bolts with different diameters. Three different failure modes were distinguished in whole set of 58 modelled specimens: block tearing, net section tearing and mixed mode. Table 3 presents only such elements, where block tearing was assigned.

Table 3. List of analysed elements, where block tearing was observed

Specimen designation	Profile	n	e_1 [mm]	p_1 [mm]	e_2 [mm]	$N_{ult,FEA}$ [kN]	$N_{EC3,2005}$ [kN]	$N_{EC3,2019}$ [kN]
A1.3	L80×5	3	70	55	41	197.01	167.67	213.40
A1.4	L90×5	3	70	55	48	221.88	182.55	228.27
A2.6	L80×5	3	70	70	41	215.42	192.61	238.34
A2.9	L80×5	4	70	50	41	214.30	182.64	239.19
A3.7	L80×5	2	70	55	46	183.66	150.86	178.30
A3.10	L80×5	3	70	55	46	216.30	178.30	224.02
A3.13	L80×5	4	70	55	46	238.78	205.73	268.22
A4.1	L60×5	2	50	70	26	119.43	104.21	131.64
A4.3	L80×5	3	30	70	41	211.53	159.36	204.4
A4.4	L80×5	3	50	70	41	215.53	175.99	221.71
A4.5	L80×5	3	90	70	41	216.22	209.24	254.97
A5.1	L100×80×5[S]	3	70	70	43	226.47	196.86	242.59
A5.2	L100×80×5[W]	3	70	70	53	251.90	218.11	263.84
A5.4	L80×60×5[W]	3	70	70	38	196.28	186.24	263.84
A5.5	L120×80×5[S]	3	70	70	45	236.37	201.11	246.84
A5.6	L120×80×5[W]	3	70	70	65	286.97	243.61	289.34
A5.8	L120×60×5[W]	3	70	70	61	267.89	235.11	280.84

W – denotes angles connected by their wider leg,
S – denotes angles connected by their smaller leg.

4. RESULTS AND DISCUSSION

4.1. OBTAINED RESULTS

The main results obtained from the analyses were as follows:

- Force-displacement curves F-Δ (Fig. 4), obtained for each connection, where F is transmitted force, and Δ is the difference between reference points P1 and P2 longitudinal displacements (Fig. 2b).
- The ultimate resistance $N_{ult,FEA}$, which was obtained as maximum force reached during loading history, from the force-displacement F-Δ curve (see Table 3).
- Distribution of effective stresses σ_{eff} (according to Huber-Mises-Hencky hypothesis) in the section under block tearing for the failure load $N_{ult,FEA}$, along two paths (subjected to tension and shear respectively). The paths definitions in which distribution of stresses were observed and examples of obtained results are shown in Fig. 5-7.

Comparing F-Δ diagrams (Fig. 4), it can be seen that elements with similar connection length but different values of bolts spacing (A2.6 i A2.9) achieved nearly the same failure load. Influence of the edge distance e_1 turned out to be insignificant. In all elements where only parameter e_1 was changed, almost the same values of $N_{ult,FEA}$ were obtained (A2.6, A4.3, A4.4 and A4.5). In unequal leg angles, the element connected by wider leg reached greater failure load and elongation (A5.1 vs A5.2 and A5.5 vs A5.6). This may be caused by different values of the edge distance e_2, which was smaller for angles joined by narrower leg. Thus net area subjected to tension was also different. Influence of this parameter is also visible when comparing elements A1.3 and A3.10.
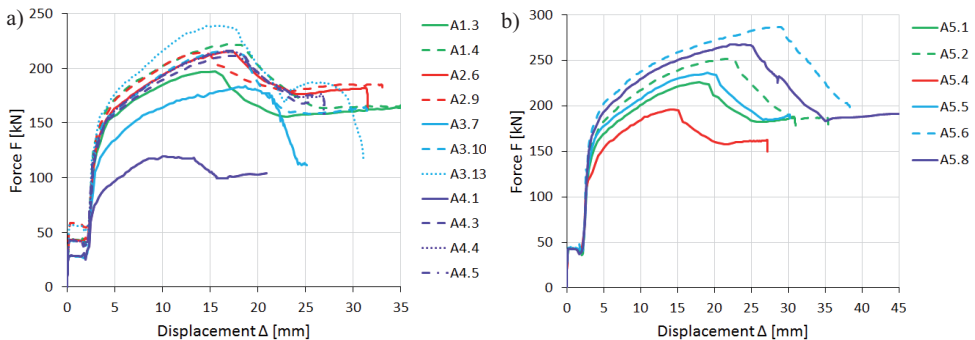

Fig. 4. Force-displacement curves: a) for equal leg angles, b) for unequal leg angles

Obtained stress distribution along shear and tension area (Fig. 6) is very similar in both possible paths of block tearing. In all cases effective stress practically reached value of f_u across the entire width of net area subjected to tension (A_{nt}). So, it can be said that stress distribution along section I-II is rather uniform and equal to ultimate stress. Values of effective stress across net area subjected to shear (A_{nv}) exceeded yield strength f_y and reached tensile strength f_u at considerable length. Effective stress across gross area subjected to shear (A_{gv}) reached and in some places exceeded yield strength f_y.

In all specimens fracture of a net area subjected to tension has occurred, similar to process of rupture presented in Fig. 3b. Fracture of shear area was not observed.
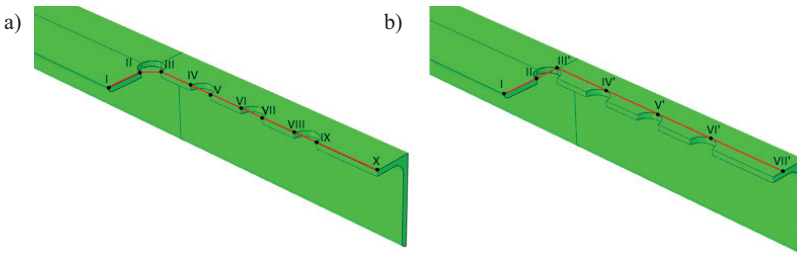
Fig. 5. Paths definitions in which distribution of stresses were observed: a) in net area subjected to shear, b) in gross area subjected to shear
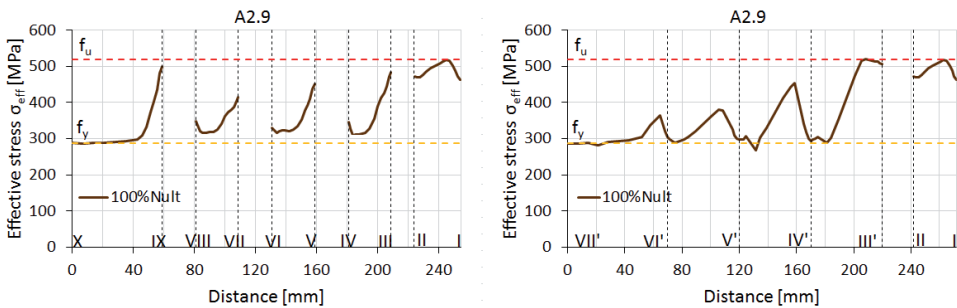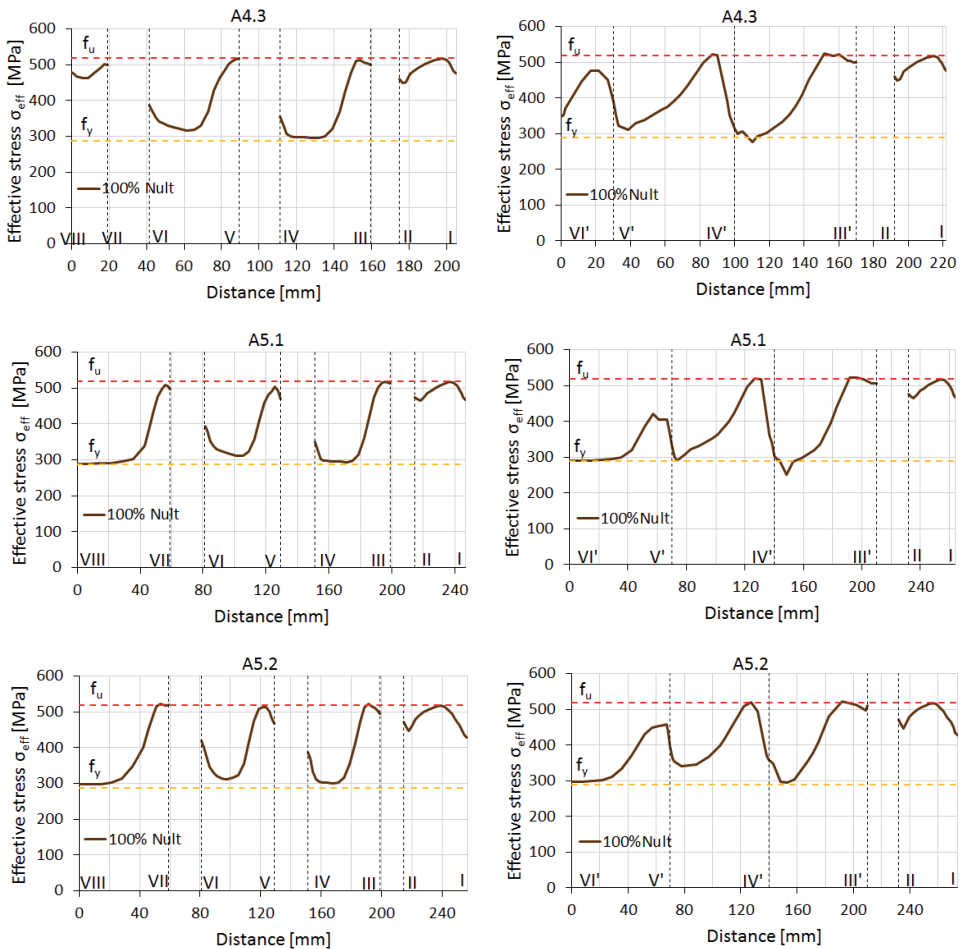
Fig. 6. Distribution of effective stresses σ_{eff} for the failure load $N_{ult,FEA}$ (left diagram shows distribution along net tension and net shear area; right one shows distribution along net tension and gross shear area)

4.2. COMPARISON OF SIMULATION RESULTS WITH EUROPEAN STANDARDS

Results presented in previous chapters were utilised to compare theoretical block tearing resistance calculated according to current version of EN 1993-1-8 [3] with new proposal prEN 1993-1-8:2019 [4]. Equations (2.1) and (2.3) were utilised in calculations, because of quasi uniform stress distribution on e_2 section. All partial factors γ_{M0} and γ_{M2} were neglected and assumed as equal to 1.0. Obtained values of theoretical resistances, marked as $N_{EC3,2005}$ and $N_{EC3,2019}$ respectively, are

presented in Table 3. Only in three elements (A2.9, A3.13 and A4.3) block tearing resistance in shear face was determined by product of A_{nv} and f_u during predictions of $N_{EC3,2019}$. The differences between simulation results and code estimations were conducted by factor calculated from Eq. (4.1). The graphic presentation of the results is shown on Fig. 7.

$$(4.1) \qquad \Delta_i = \left(N_{EC3,i} - N_{ult,FEA}\right)/N_{ult,FEA}$$

where: $N_{EC3,i}$ is equal to $N_{EC3,2005}$ or $N_{EC3,2019}$ respectively.
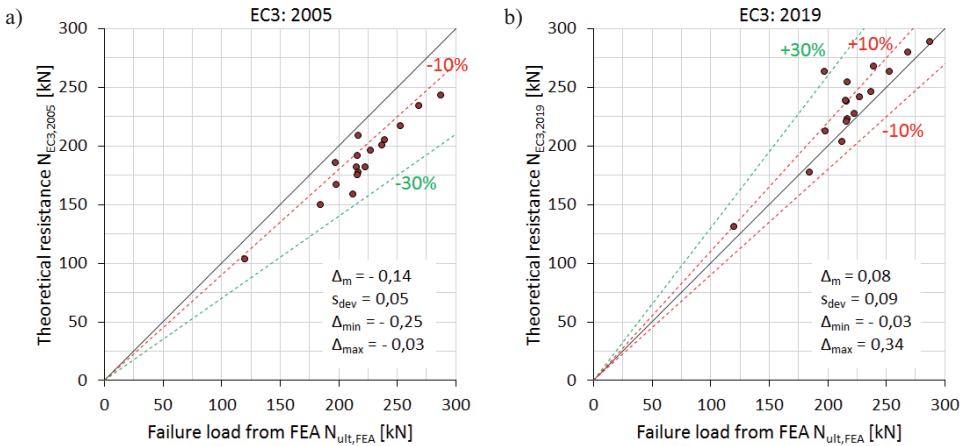
Fig. 7. Comparison of theoretical block tearing resistance with ultimate resistance obtained from numerical simulations $N_{ult,FEA}$: a) for current Eurocode 3 [3], b) for new proposal [4]

A positive or negative value of Δ_i means that ultimate resistance calculations using EC3 formulas give respectively higher or lower values than the failure load determination from FE analyses. The mean values of calculated factor Δ_m, its standard deviation s_{dev}, maximum and minimum values of factor Δ_i are presented in Fig. 7 for each reference group. It can be seen that mean value of calculated factor Δ_m is slightly closer to zero for the newest proposal (prEN 1993-1-8:2019 [4]), but the current version of Eurocode is characterized by more likely resistance prediction (with slightly smaller standard deviation s_{dev}).

5. CONCLUSIONS

Paper presents finite element analysis of block tearing failure in steel angles connected by one leg. Numerical simulations are based on Gurson-Tvergaard-Needleman porous material model and show that such approach can accurately trace the behaviour of the steel joints at plastic and ultimate range. The computational model was validated using own test results.

Based on the analysis, the following conclusions can be formulated:

- The ultimate resistance of single angle in tension connected by a single row of bolts in one leg is often governed by block tearing resistance.

- In such case, fracture of the net area subjected to tension occurs first. Shear area is heavily stressed, but fracture in this region has not been observed, neither during tests, nor numerical analysis. Its occurrence after forming a crack in tension area is rather impossible, because the remainder part of cross section is then subjected to bending, which causes important redistribution of internal forces.

- Observations of stress distribution for the failure load show that contribution of shear plane to block tearing resistance is limited by plastic resistance of gross area and ultimate resistance of net area, which is consistent with the newest code provisions [4].

- Block tearing resistance formulas proposed in the newest version of Eurocode 3 [4] give slightly better agreement with the results obtained from FE analysis.

REFERENCES

1. E. Bernatowska, L. Ślęczka, "Net section fracture assessment of steel bolted joints with shear lag effect" MATEC Web of Conferences 262, 2019.
2. P. C. Birkemoe, M. I. Gilmor, "Behavior of Bearing Critical Double-Angle Beam Connections", Engineering Journal, AISC, Vol. 15 (1978), pp. 109-115.
3. EN 1993-1-8:2005: Eurocode 3 – Design of steel structures –part 1-8: Design of joints. CEN, Brussels, 2005.
4. prEN 1993-1-8:2019: Eurocode 3 – Design of steel structures – part 1-8: Design of joints. CEN/TC250, 2019.
5. M. B. Helwe, S. N. El Kalash, E. G. Hantouche "Alternate block shear in beams: Experimental and FE fracture modeling", Engineering Structures 186 (2019) 110–120.
6. J. Kim, J. Yoon, B. Kang, "Finite element analysis and modeling of structure with bolted joints", Applied Mathematical Modelling 31: 895–911, 2007.
7. P. Kossakowski, "An analysis of the load-carrying capacity of elements subjected to complex stress states with a focus on the microstructural failure". Archives of Civil and Mechanical Engineering 10: 15-39, 2010.
8. P. Kossakowski, "Analysis of the void volume fraction for S235JR steel at failure for low initial stress triaxiality", Archives of Civil Engineering 64:101-115, 2018.
9. P. Kossakowski, „Application of damage mechanics in the analysis of pre-failure states of metal structures" (in Polish), Zeszyty Naukowe Politechniki Rzeszowskiej Budownictwo i Inżynieria Środowiska 59 (3/12/II): 177-184, 2012.
10. G. L. Kulak, E. Y. Wu, "Shear lag in bolted angle tension members", Journal of Structural Engineering, vol. 123, pp. 1144-1152, 1997.

11. P. Može, "Angles connected by one leg in tension", EUROSTEEL 2017, September 13–15, 2017, Copenhagen, Denmark.

12. H. L. N. Munter, L. P. Bouwman, "Report: 6-81-21: Angles connected by bolts in one leg, Comparison to French, Eurocode 3 and Dutch formulae with the results of French and Dutch tests", Stevin Laboratory, Department of Civil Engineering, Delft University of Technology, November 1981.

13. E. L. Salih, L. Gardner, D. A. Nethercot, "Numerical investigation of net section failure in stainless steel bolted connections", Journal of Constructional Steel Research, 66: 1455-1466, 2010.

14. H. H. Snijder, D. Ungermann, J. W. B. Stark, G. Sedlacek, F. S. K. Bijlaard, A. Hemmert-Halswick, "Evaluation of test results on bolted connections in order to obtain strength functions and suitable model factors - Part A: Results. Eurocode No.3 - Part 1 - Background documentation", Commission of the European Communities, Brussels 1988.

15. H. H. Snijder, D. Ungermann, J. W. B. Stark, G. Sedlacek, F. S. K. Bijlaard, A. Hemmert-Halswick, "Evaluation of test results on bolted connections in order to obtain strength functions and suitable model factors - Part B: Evaluations." Eurocode No.3 - Part 1 - Background documentation, Commission of the European Communities, Brussels 1988.

16. C. Topkaya, "A finite element parametric study on block shear failure of steel tension members", Journal of Constructional Steel Research 60: 1615-1635, 2004.

17. H. Wen, H. Mahmoud, "Simulation of block shear fracture in bolted connections", Journal of Constructional Steel Research 134: 1-16, 2017.

LIST OF FIGURES AND TABLES:

Tab. 2. The range of experimental tests compared with FE modelling

Tab. 2. Zakres badań eksperymentalnych porównywanych z modelem MES

Tab. 3. List of analysed elements, where block tearing was observed

Tab. 3. Lista analizowanych elementów, gdzie zaobserwowano rozerwanie blokowe

ANALIZA NUMERYCZNA ROZERWANIA BLOKOWEGO W KĄTOWNIKACH POŁĄCZONYCH JEDNYM RAMIENIEM

Słowa kluczowe: *połączenia śrubowe, rozerwanie blokowe, analiza MES, model materiału Gursona-Tvergaarda-Needlemana, stalowe kątowniki*

STRESZCZENIE:

Rozerwanie blokowe w połączeniach śrubowych następuje przez jednoczesne ścięcie przekroju netto wzdłuż kierunku obciążenia i rozerwanie przekroju netto w jego poprzek. Ocenia się, że jest ono miarodajne w wielu przypadkach przy wyznaczaniu nośności kątowników mocowanych jednym ramieniem przy użyciu śrub. Istnieje wiele badań doświadczalnych tego zjawiska, lecz liczba analiz numerycznych rozpatrujących tę formę zniszczenia nie jest duża.

W niniejszej pracy zawarto opis modelu połączenia śrubowego, zbudowanego za pomocą MES, którego celem jest analiza rozerwania blokowego występującego w kątownikach. Model zawiera wszystkie elementy składowe połączenia, takie jak blacha węzłowa, kątownik, śruby z nakrętkami i podkładki. Uwzględnione jest zjawisko kontaktu, co pozwala właściwie odwzorować przekazywanie sił przez śruby podlegające dociskowi. Zastosowano sprężysto-plastyczny model materiału Gursona-Tvergaarda-Needlemana, który ujmuje proces niszczenia materiału. Taki model materiału pozwala na szacowanie obciążenia granicznego spowodowanego plastycznym jego pękaniem, z uwzględnieniem parametrów mikrostruktury oraz właściwości mechanicznych. Właściwości mechaniczne zastosowanej stali uzyskano z badań. Pozostałe parametry determinujące proces niszczenia zaczerpnięto z piśmiennictwa oraz procesu kalibracji modelu materiału. Własne badania doświadczalne połączeń kątowników mocowanych jedną, lub większą liczbą śrub (od 2 do 4), posłużyły także do walidacji zachowania całego połączenia. Walidacja została przeprowadzona na podstawie zarówno globalnego, jak i lokalnego zachowania połączenia.

Zbudowany model został użyty do przeprowadzenia analizy parametrycznej. Ogółem zbudowano 58 modeli połączeń, w których badano wpływ następujących parametrów:

- stosunku szerokości ramienia do jego grubości b/t w kątownikach równoramiennych,

- rozstawu otworów na śruby w kierunku działania obciążenia p_1 i całkowitej długości połączenia,

- odległości osi otworu od krawędzi w kierunku prostopadłym do kierunku działającego obciążenia e_2,

- odległości osi skrajnego otworu od krawędzi e_1,

- łączenia szerszym lub węższym ramieniem w przypadku kątowników nierównoramiennych,

Głównymi wynikami otrzymanymi z tych analiz, były zależności siła-wydłużenie, nośność graniczna i forma zniszczenia. Odczytywano także rozkład naprężenia w przekrojach podlegających zniszczeniu blokowemu. Dla tych elementów, w których otrzymano zniszczenie przez rozerwanie blokowe, wyniki posłużyły do porównania dwóch podejść obliczeniowych – oceny nośności według aktualnej normy PN-EN 1993-1-8 oraz według propozycji jej nowelizacji prEN 1993-1-8.